S-Band Klystron with 300 MHz Bandwidth at 850 kW Peak Power and 20 kW Average Power

Zhiqiang Zhang[1, *], Jirun Luo[1, 2, *], Zhaochuan Zhang[1], Xiaojuan Yu[1], and Yunping Huang[1]

Abstract—In this paper, an S band, 300 MHz bandwidth, and 20 kW average power klystron was developed in the Aerospace Information Research Institute, Chinese Academy of Sciences. The klystron operates at 72 kV beam voltage and 41 A beam current with peak powers of over 850 kW and efficiency of over 30% at a 2.47% RF duty cycle. The results, including simulations, design, technologies, and performances of the klystron, are presented. Some problems such as gain dip, high order mode oscillation, output window cracking, and startup time were also discussed.

1. INTRODUCTION

With the development of new technologies, such as steered phased array and simultaneous multiple beams, radar systems have experienced a period of development at top speed in recent 30 years. However, at the same time, the observed targets also made progresses in some areas such as multiple targets, miniaturization, high speed, and stealth. In addition, interferential technologies which aim at radar systems have been developed rapidly. So, as a core device in the radar transmitter, expanding bandwidth and increasing average power of the klystron are the two trends to satisfy the requirements of anti-interference and force. In the past three decades, some research organizations in USA, France, Britain, and China have developed some broadband klystrons with the bandwidth about 10%–15% in S or C band and 5%–10% in X band, which corresponds to VKS8340 at CPI, PT6120 at TMD, TH2092 at TED, and KS4058 at IECAS [1–3]. The levels of high average power klystrons have been achieved about 1.3 MW in P band, 1.2 MW in L band, 500 kW in S band, and 50 kW in X band. Typical examples are LEP at SLAC, E3718 at Toshiba, VKS7269 at CPI, and PT6203 at TMD [4, 5]. The klystron presented in this paper can realize larger than 10% instantaneous bandwidth with the output peak power of 850 kW and output average power of 20 kW at 72 kV beam voltage and 41 A beam current.

The required performance specifications for the klystron are shown in Table 1.

2. DESIGN

According to the parameters in Table 1, there are two key points for developing the klystron. One is how to obtain over 10% relative bandwidth at a relatively low output peak power level, and the other is a electron gun assembly for keeping not less than 5000 hours lifetime with 5 minutes startup time. So the design will mainly focus on solving the above two problems so that one can choose appropriate size of the cathode, the number and structure of buncher, and output section circuit.

Table 1. Required performance specifications.

parameters	value
Frequency	S band
Average power/kW	≥ 20
Peak Power/kW	≥ 850
Bandwidth/MHz	≥ 300
Efficiency/%	≥ 30
Saturated Gain/dB	≥ 40
Beam voltage/kV	≤ 75
Beam current/A	≤ 45
RF pulse width/μs	95
Duty cycle/%	2.47
Focusing	Solenoid
Lifetime/h	≥ 5000
Startup time/min	~ 5

2.1. Electron Gun and Electron Trajectories

To obtain the bandwidth of over 10% at the 850 kW output peak power level, a high perveance electron gun of 2.2 μp is selected in the range of appropriate size and current density of the cathode. The simulated results of the cathode parameter using Arsenal code are shown in Fig. 1. The left figure in Fig. 1 illustrates that with the increasing of the iteration number, the perveance gradually reaches a stable value about 2.2 μp. The right figure in Fig. 1 shows that the current density is about 1 A/cm^2 at the center and about 2 A/cm^2 at the edge. These parameters indicate that the emission characteristic of the cathode is relatively uniform.

```
Vo    =0.7500E+02 kV      Io    =0.4522E+02  A      Po   =0.3391E+04 kW
Rbeam=0.5246E+00 cm       Rbo   =0.0000E+00 cm      Emtnc=0.0000E+00 rad*cm
vo/c =0.4895E+00          Rtube=0.8000E+00 cm       Bo   =0.1627E+04 Gs
Gamma=0.1147E+01          Perv =0.2201E+01          Lo   =0.1000E+01 cm
```
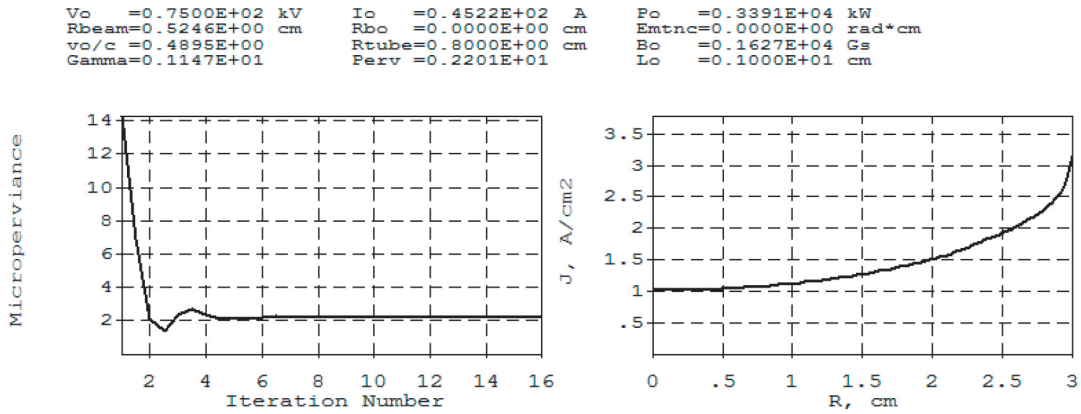

Figure 1. The cathode parameters.

To achieve the objective of 5000 hours lifetime, the current density of the barium-tungsten cathode cannot be too large, so the diameter of the cathode is designed as 52 mm (shown in Fig. 2), and current density is only about 2 A/cm^2 to satisfy the requirements of 5000 hours lifetime.

In order to attain the objective of 5 minutes startup time, the thickness of the barium-tungsten cathode is designed as 2 mm, and 6 layers of the molybdenum thermal shielding cases are used in the electron gun assembly to increase the thermal efficiency. W-Re (W: 75%, Re: 25%) is utilized as the heater material. In heating process for the electron gun assembly in a dynamic vacuum system, its

Table 2. The result of thermal testing.

1′42″	1′56′	2′15″	2′48″	3′42″	4′30
800°C	850°C	900°C	950°C	1000°C	1050°C

temperature was tested by an infrared-pyrometer. The tested results are given in Table 2, which shows that the temperature of the cathode can achieve 1000°C after it is heated 3 minutes and 42 seconds. Because the current density for cathode operation is only about $1\,\mathrm{A/cm^2}$ at the center and $2\,\mathrm{A/cm^2}$ at the edge, the temperature of 1000°C can ensure that the cathode operates normally, so the electron gun can satisfy the requirement of 5 minutes startup time.

From the cathode lifetime versus cathode loading curves (shown in Fig. 3), one can see that when the cathode current is lower than $10\,\mathrm{A/cm^2}$, the cathode lifetime can be over 10000 hours easily. The cathode used in the klystron is composed with the porous tungsten of 28%–30% porosity, a mixture of $6\mathrm{BaO}{:}1\mathrm{CaO}{:}2\mathrm{Al_2O_3}$, and W-Re-Os alloy film. It can be seen from Fig. 4 that using W-Re-Os alloy film instead of Os-W can increase the emission ability of the cathode under the condition of high voltage.

Based on the above-mentioned parameters, the sizes, shapes, and relative positions of the cathode, anode, and focusing electrode in the electron gun are obtained through simulating and optimizing the static electron trajectory without and with focusing magnetic field in the klystron. The optimized result without focusing magnetic field is shown in Fig. 5. One can see clearly from Fig. 5 that the laminar flow of the electron beam is satisfactory.

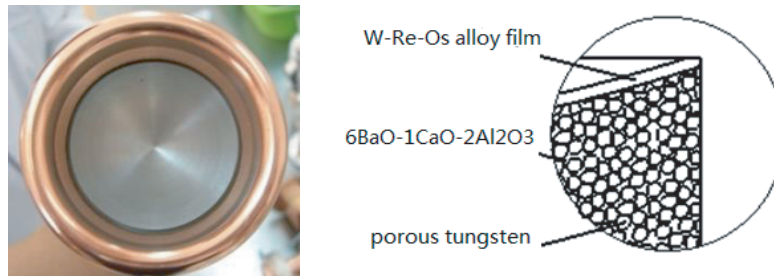The static electron trajectory with focusing magnetic field in the klystron is shown in Fig. 6. One

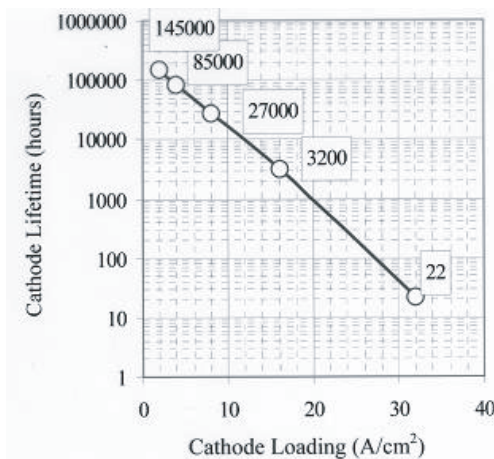**Figure 2.** The cathode appearance and its structure.

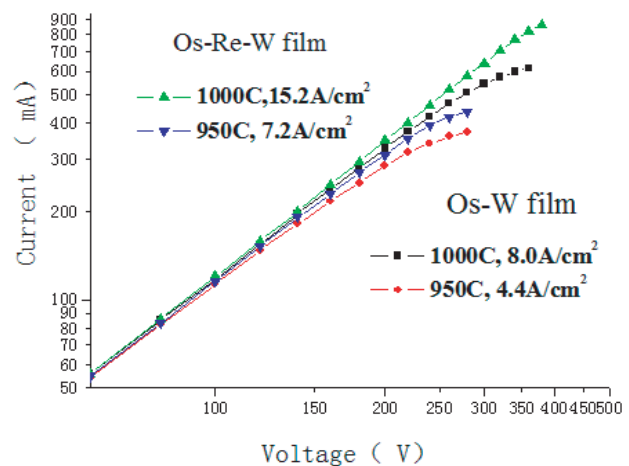**Figure 3.** Cathode lifetime versus the cathode loading.

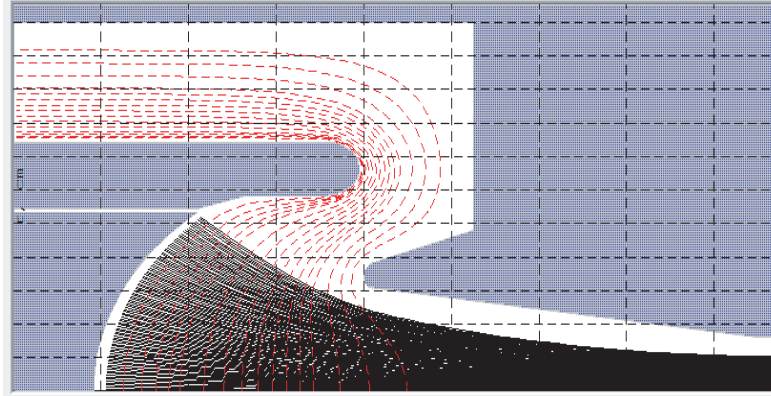**Figure 4.** Comparison of the emission ability of the cathodes coated with two kinds of alloy films.

Figure 5. The static trajectory of the electron beam without focusing magnetic field.
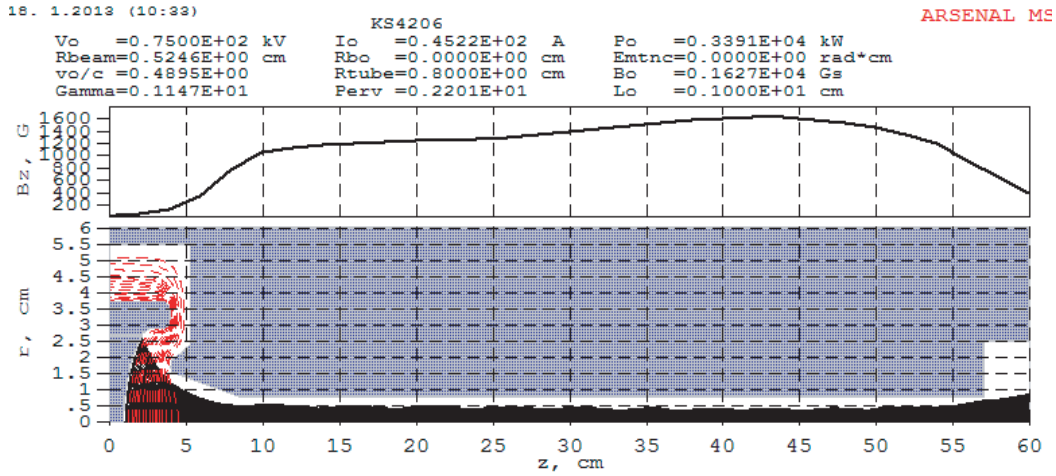

Figure 6. The dynamic trajectory of the electron beam with focusing magnetic field.

can see from Fig. 6 that the average radius of the electron beam is only about 5.2 millimeters. Because the drift radius is designed as 8 millimeters, the filled factor (b/a) is about 0.65 to keep the electron beam transmission good.

2.2. Output Circuit

To acquire the 300 MHz bandwidth, an over-lapping mode double-gap output circuit is adopted [6–8]. In this structure, cavity 1 and cavity 2 couple each other through the coupled slot. The distance L between the two cavity gaps is selected according to the equation $\beta_e L = 235°$ to ensure the high efficiency and stability of the klystron. The structure and equivalent circuit are shown in Fig. 7 and Fig. 8. Fig. 9 gives the designing curves of the real part of the impedance versus the frequency for the equivalent circuit, which means that a bandwidth over 10% can be reached.

In a klystron, high perveance is helpful for improving the bandwidth, but this will count against achieving the efficiency. To meet the demand of the bandwidth of the buncher, 8 cavities are distributed in the buncher region, and the first seven cavities have been loaded by microwave attenuating materials to decrease the Q of the cavity and enhance the bandwidth. The geometrical and electrical parameters of the beam-wave interaction were optimized using the 2.5-D Arsenal-MSU code [9] to reach the specification related to the output power, efficiency, and gain list in Table 1. The distribution of the frequencies and Q values, and R/Q for the cavities in the buncher is shown in Table 3.
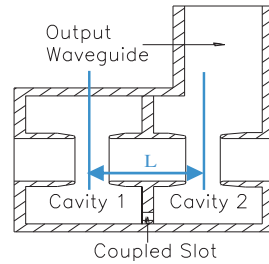
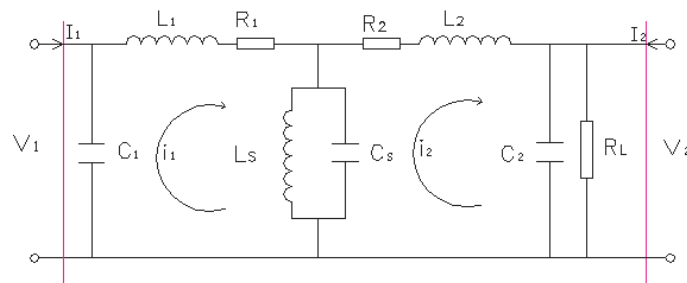**Figure 7.** The structure of an over-lapping mode double-gap output system.

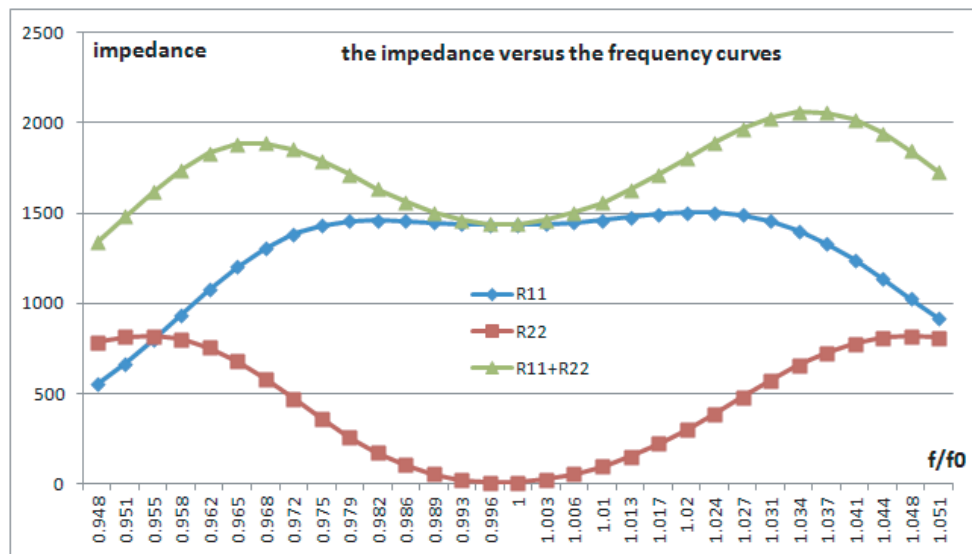**Figure 8.** The equivalent circuit of an over-lapping mode double-gap output system.

Figure 9. The real part of the impendence of an over-lapping mode double-gap output circuit.

3. EXPERIMENTAL RESULTS

Based on above-mentioned simulated and optimized parameters and some improving processes, four experimental tubes have been designed, manufactured, and tested to obtain good output characteristics and stability [10]. In the testing process for the first experimental klystron, we found that when the frequency of the input RF signal was $0.962f_0$, the output pulse waveform on the oscilloscope dithered, and the amplitude of the pulse rear end was obviously lower than that of the pulse foreside. At the same time, the measured RF output power sharply dropped, and vacuum became worse in it. Sometimes, the vacuum deterioration caused the voltage of the pulse modulator automatically to be cut down because

Table 3. The frequencies and Q values of the cavities.

Cavity No.	Frequency (f/f_0)	Q	R/Q
1	0.976	30	105
2	0.948	50	105
3	0.959	50	105
4	1.021	35	110
5	1.048	70	110
6	1.055	75	110
7	1.069	130	110
8	1.076	2000	110
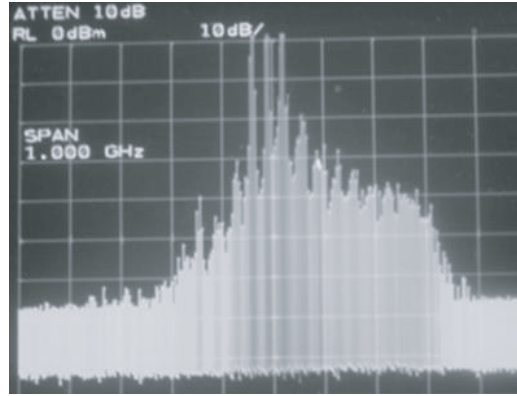
Figure 10. The output spectrum of the frequency of $0.962f_0$.

of over large ion current going through the titanium pump, which stopped the operation of the klystron. As can be seen from Fig. 10, the output spectrum was not pure, and the noisy signal was amplified. In addition, the second harmonic of the input signal was also amplified, and its amplitude was almost as high as that of the first harmonic on spectrum analyzer. However, when the frequency of the input signal departed ± 0.01 GHz from $0.962f_0$, the output power recovered the normal value, and the spectrum also obtained obvious improvement.

Through simulation with HFSS code and cold testing for the cavities unloading microwave attenuating material in the buncher, we found that there was a high-order mode (TM_{011}) whose frequency was equal to the second harmonic frequency of $0.962f_0$. In order to suppress the oscillation of the high-order mode and keep the output characteristics of the klystron for the other frequencies, we try to adjust the size of the 8th cavity geometrical structure to make the resonant frequency of the high-order mode depart from the second harmonic frequency of the fundamental mode and nearly not affect the resonant frequency of the fundamental mode. The calculations and cold testing found that when h increased, and r decreased in the cavity model (Fig. 11) at the same time according to a proper manner, the size variation had little influence on the frequency of the fundamental mode, but had more influence on the frequency of the high-order mode.

Based on the improved cavity, the second experimental klystron was manufactured. There was no any parasitical oscillation in the operational frequency band of the klystron in the power testing process. Its output spectrum at the frequency of $0.962f_0$ on spectrum analyzer is as shown in Fig. 12. However, the testing found that there was a dip of the output power and gain for the klystron near the frequency of $1.031f_0$. Fig. 13 gives the curve of the gain versus frequency, which shows that the gain in the frequency range of 1.024–$1.051f_0$ is less than 40 dB. Any change for the input power or focusing magnet field will all make the output power and gain further decrease. The output power
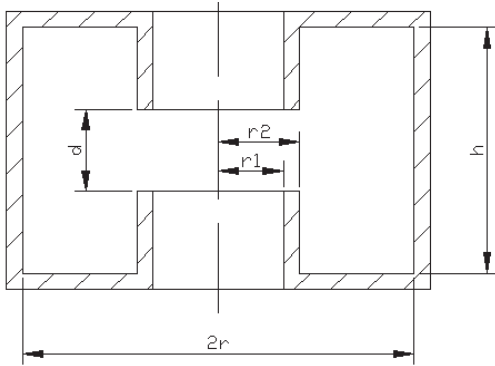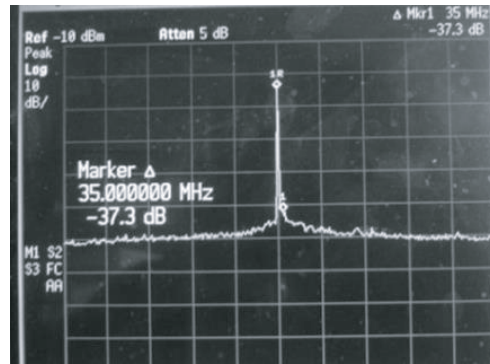
Figure 11. The model of reentrant cavity.

Figure 12. The output spectrum of the frequency of $0.962f_0$ tested on the improved klystron.
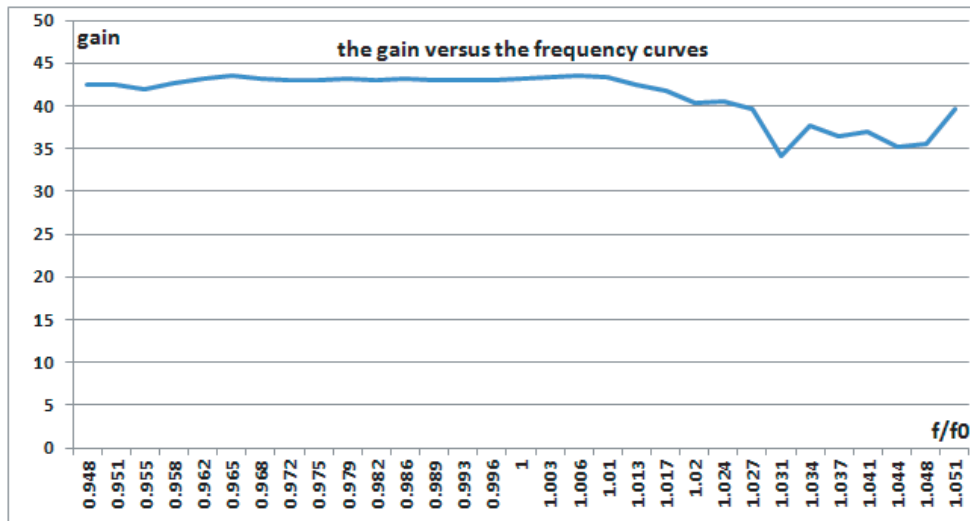

Figure 13. The gain dip curves.

versus frequency trend of the klystron was confirmed with the 2.5-D Arsenal-MSU code, which is good agreement with the test results [11]. We tried to adjust the frequencies of some cavities and the gap distance between the adjacent cavities for improving the bunching and increase the gain in the frequency range of 1.024–$1.051f_0$. However, the results calculated with the 2.5-D Arsenal-MSU code showed that the gain could be compensated in the high frequency range except near $1.031f_0$. So a low Q cavity was added at the frequency of $1.031f_0$ between the fourth cavity and fifth cavity. The simulating result is that the gain curve can reach larger than 40 dB in the whole operating frequency band by adjusting the gap distances between the adjacent cavities at the Q value of 40 for the added cavity without the variation of the whole interaction length for the klystron. The improved gain curve versus frequency is shown in Fig. 14 using 9 cavities as the buncher.

The third experimental klystron was designed and manufactured based on the new structure parameters with 9 cavities as the buncher. The tested results show that the output peak power of $889 \sim 926$ kW with the efficiency larger than 30%, -1.5 dB bandwidth over 300 MHz, gain larger than 40 dB, and average power larger than 20 kW can be reached at an RF pulse width of 95 μs, a repetition rate of 260 Hz, beam voltage of 72 kV, beam current of 41 A, minimum DC (Direct Current), and RF beam transmission rates of 98% and 94%. Table 4 gives the tested results of the klystron, which means that the output performances have met the requirement for the design. However, the output window cracked during the aging process for testing the stability and reliability of the output performances for

Table 4. The measured result of the klystron.

Frequency (MHz)	Input power (W)	Output power (kW)	Efficiency (%)	G (dB)
$f_0 - 150$	66	889	30.1	41.2
$f_0 - 120$	55	895	30.3	42.1
$f_0 - 90$	75	917	31.1	40.9
$f_0 - 60$	71	917	31.1	41.1
$f_0 - 30$	54	909	30.8	42.3
f_0	50	909	30.8	42.6
$f_0 + 30$	32	926	31.4	44.6
$f_0 + 60$	57	922	31.2	42.1
$f_0 + 90$	86	900	30.5	40.2
$f_0 + 120$	88	891	30.2	40.1
$f_0 + 150$	85	889	30.1	40.1

the klystron at the input signal frequency of $0.976 f_0$, and the klystron was broken with a tremendous noise from the output waveguide.

We carefully checked the crack in the failed window disk and found that there was no obvious pollution on the vacuum-side/air-side surface of the window, and the direction of the crack was in good agreement with that of the maximum E-field of the TE_{11} cylindrical-guide mode. A photograph of the cracked window disk is shown in Fig. 15. So we think that the power capacity of the window is enough to 20 kW average power because of no obvious pollution on the surface of the window, and the crack may be caused by high electric field breakdown, which means that there may be a high Q value oscillation mode in the output window.

Based on the above-mentioned analysis, the simulation with HFSS code and cold testing with network analyzer were simultaneously done in detail for the window to check if there was any oscillation mode in it. The cold testing finds that a oscillation mode may appear when the centric axes of two section rectangular waveguides and a cylindrical waveguide in the middle (Fig. 16) are not on the same line (caused by machining errors), whose frequency is $0.976 f_0$. The calculation with HFSS code for
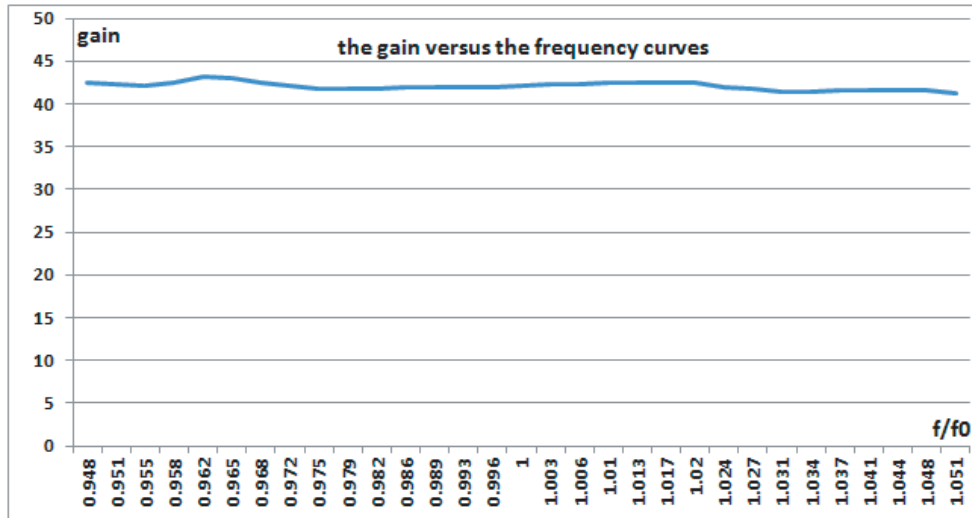
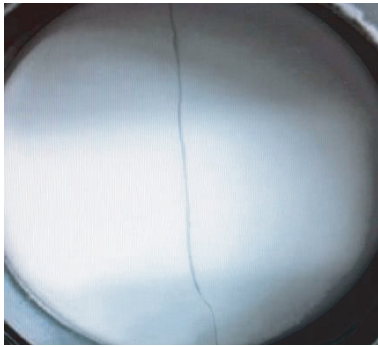**Figure 14.** Gain curves after improvement.
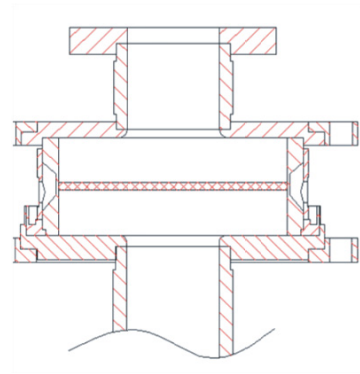
Figure 15. The crack window.

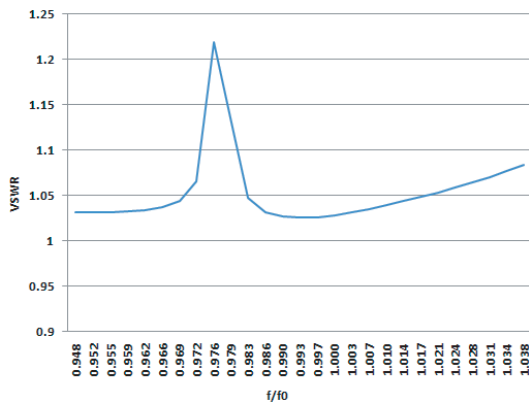**Figure 16.** The structure of the window.

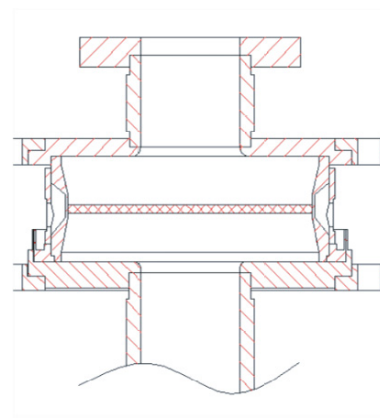**Figure 17.** The calculated result with HFSS of the window.

Figure 18. The adjusted structure of the window.

the same window structure model is also in good agreement with the cold testing (shown in Fig. 17) Because controlling machining errors is not so easy like changing the design of the window structure, we hope to reduce the oscillation mode frequency to less than the lowest operating frequency. An improvement for the pillbox window structure is shown in Fig. 18, and the simulation with HFSS code was performed. The result shows that the oscillation frequency becomes $0.931f_0$, which is lower than the lowest operating frequency of $0.948f_0$, and the performances for the bandwidth and transmission all meet the design requirement. Cold testing further demonstrates the simulation results. So the fourth experimental klystron was manufactured according to the improved parameters, and the results for testing and aging show the electric performances, stability, and reliability which all meet the required specifications.

4. CONCLUSION

An S-band klystron with 300 MHz bandwidth, 850 kW output peak power, 20 kW average power, and efficiency of over 30% has been developed at 72 kV beam voltage and 41 A beam current with 2.47% RF duty cycle through adjusting the size of the unloaded cavity to suppress the high order mode oscillation, adding a buncher cavity to eliminate the gain dip, lowering the resonant frequency of the parasitical oscillation mode in the output window to less than the minimal operational frequency to avoid output window cracking as well as reducing the thickness of the cathode, improving heating efficiency, and changing the heater's material to realize 5 minutes startup time.

REFERENCES

1. Saman H. A. and G. P. Saraph, "Design analysis of broadband output circuits for klystron amplifiers," *Conf. Rec. 31st IEEE Int. Conf. Plasma Sci.*, 217, 2004.

2. Ding, Y. and Y. Zhu, "Studies on broadband output circuit of high power klystron," *Proc. Int. University Conf. Electronics Radiophys. Ultra-High Frequencies*, 383, St. Petersburg, Russia, 1999.

3. Delu, N. and D. Yaogen, "A ten percent bandwidth high power pulsed klystron amplifier," *J. Electronics*, Vol. 5, 197, May 1983 (in Chinese).

4. Yong, W., Y.-G. Ding, P.-K. Liu, J. Zhang, S.-G. Wang, and X. Lu, "Development of an S-band klystron with bandwidth of more than 11%," *IEEE Trans. Plasma Sci.*, Vol. 34, 572, 2006.

5. Wang, Y., Y. Ding, P. Liu, Z. Zhang, and J. Zhang, "Research progress of S-band broadband klystron in IECAS," *2010 IEEE International Vacuum Electronics Conference*, 219, Monterey, California, May 2010.

6. Zhang, Z. C., J. J. Fan, Y. W. Zhang, R. M. Wang, Y. F. Guo, F. Zhu, and C. J. Fu, "Development of a C-band klystron with a 360-MHz instantaneous bandwidth," *IEEE Trans. on Electron Devices*, Vol. 57, 3485, 2010.

7. Xiu, L., Y.-L. Zhang, Y.-H. Wang, Y.-J. Tao, Q. Wang, J. Wang, X.-H. Zuo, Y. Dou, and F. Luo, "A 500 kW C-band broadband klystron," *2008 IEEE International Vacuum Electronics Conference*, 205, Monterey, California, April 2008.

8. Lin, F., Y. Ding, and Z. Zhang, "Simulation computation method for calculating the impedance matrix of double gap cavity of klystron," *Journal of Electronics and Information Technology*, Vol. 26, 1480, 2004 (in Chinese).

9. Sandalov, A. N., "Animation of nonlinear electron-wave interaction in klystron," *RF'96, Pulse RF Sources for Linear Colliders*, 8, Stanford, California, 1996.

10. Lin, F. and Y. Ding, "Criterion of absolute stability of output circuit with coupling two gap cavity of klystron," *Vacuum Electronics*, Vol. 2, 10, 2004 (in Chinese).

11. Gao, D., Y. Ding, Z. Zhang, B. Shen, Z. Zhang, J. Cao, H. Gu, C. Wang, and F. Wang, "Progress of S-band high average power broadband multi-beam klystron," *2014 IEEE International Vacuum Electronics Conference*, 117, Monterey, California, 2014.